Chemical Force Microscopy: Exploiting Chemically-Modified Tips To Quantify Adhesion, Friction, and Functional Group Distributions in Molecular Assemblies

Aleksandr Noy,[†] **C. Daniel Frisbie,**[†] **Lawrence F. Rozsnyai,**[‡]
Mark S. Wrighton,[‡] **and Charles M. Lieber**[*,†]

*Contribution from the Department of Chemistry and Division of Applied Sciences, Harvard
University, Cambridge, Massachusetts 02138, and Department of Chemistry, Massachusetts
Institute of Technology, Cambridge, Massachusetts 02139*

Abstract: Chemical force microscopy (CFM) has been used to measure adhesion and friction forces between probe tips and substrates covalently modified with self-assembled monolayers (SAMs) that terminate in distinct functional groups. Probe tips have been modified with SAMs using a procedure that involves coating commercial Si_3N_4 cantilever/tip assemblies with a thin layer of polycrystalline Au followed by immersion in a solution of a functionalized thiol. This methodology provides a reproducible means for endowing the probe with different chemical functional groups. The spring constants and radii of the chemically modified cantilever/tip assemblies have been characterized to allow for quantitative friction and adhesion measurements. Au-coated Si and Si substrates have been treated with functionalized thiols and silanes, respectively, to produce SAM coated substrates terminating with different functional groups. A force microscope has been used to characterize the adhesive interactions between probe tips and substrates that have been modified with SAMs which terminate with COOH, CH_3, and NH_2 functional groups in EtOH and H_2O solvents. Force vs distance curves recorded under EtOH show that the interaction between functional groups decreases as follows: $COOH/COOH > CH_3/CH_3 > COOH/CH_3$. The measured adhesive forces were found to agree well with predictions of the Johnson, Kendall, and Roberts (JKR) theory of adhesive contact and thus show that the observed adhesion forces correlate with the surface free energy of the molecular groups in EtOH. Electrostatic contributions to adhesive forces have also been studied using a COO^-/NH_3^+ tip/surface in aqueous solution. Force vs distance curves recorded as a function of ionic strength show that the observed adhesive interaction decreases with increasing ionic strength. These results have been interpreted in terms of contact and noncontact contributions to the experimentally measured adhesive force. The friction forces between tips and samples modified with COOH and CH_3 groups have also been measured as a function of applied load. The magnitude of the friction force was found to decrease in the following manner with different tip/sample functionalities: $COOH/COOH > CH_3/CH_3 > COOH/CH_3$. Friction forces between different chemical functional groups thus correlate directly with the adhesion forces between these same groups. Specifically, high friction is observed between groups that adhere strongly, while low friction is observed between weakly interacting functional groups. The dependence of friction forces on the tip and sample functionality is shown to be the basis for chemical force microscopy in which lateral force images are interpreted in terms of the strength of both adhesive and frictional interactions between different functional groups.

Introduction

Intermolecular forces are responsible for a wide variety of phenomena in condensed phases extending from capillarity and lubrication at macroscopic length scales, through micelle and membrane self-assembly on a mesoscopic scale, to molecular recognition and protein folding at the nanoscopic scale.[1] Development of a fundamental understanding of such important phenomena, regardless of the length scale, requires detailed knowledge of the magnitude and range of intermolecular forces. For example, macroscopic measurements of friction and adhesion between surfaces are influenced by complex factors such as surface roughness and adsorbed contaminants. Microscopic studies of these forces should, however, be interpretable in terms of fundamental chemical forces such as van der Waals, hydrogen

bonding, and electrostatic interactions. In addition, an understanding of intermolecular forces in condensed phases is of significance to nanoscale chemistry where noncovalent interactions are important to the manipulation, assembly, and stability of new nanostructures.

Direct experimental measures of the interactions between molecules and molecular assemblies can be achieved using several techniques, including the surface forces apparatus (SFA),[2] optical tweezers,[3] and scanning force microscopy.[4–9] The SFA has yielded considerable information about adhesion and friction between molecular assemblies, although these data

† Harvard University.
‡ Massachusetts Institute of Technology.
⊗ Abstract published in *Advance ACS Abstracts*, July 15, 1995.
(1) (a) Israelachvili, J. *Intermolecular & Surface Forces*; Academic Press: New York, 1992. (b) Ulman, A. *Introduction to Ultrathin Organic Films*; Academic Press: New York, 1991. (c) Fersht, A. *Enzyme Structure and Mechanics*; W. H. Freeman: New York, 1985.

(2) (a) Israelachvili, J. *Acc. Chem. Res.* **1987**, *20*, 415. (b) Yoshizawa, H.; Chen,Y.-L.; Israelachvili, J. *J. Phys. Chem.* **1993**, *97*, 4128. (c) Chen, Y.-L.; Helm, C. A.; Israelachvili, J. *J. Phys. Chem.* **1991**, *95*, 10736. (d) Israelachvili, J. *J. Vac. Sci. Technol.* **1992**, *10*, 2961.
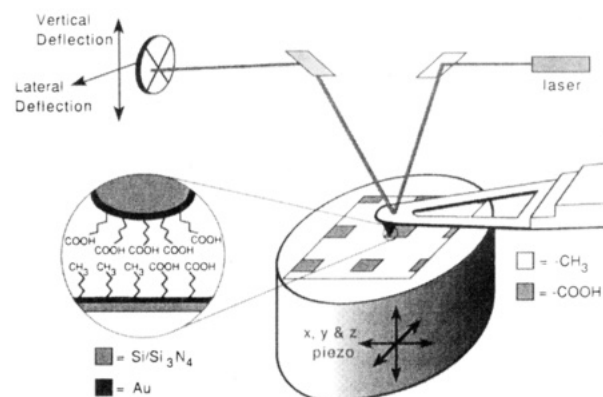
(3) (a) Ashkin, A.; Dziedzic, J. M.; Bjorkholm, J. E.; Chu, S. *Optics Lett.* **1986**, *11*, 288. (b) Kuo, S. C.; Sheetz, M. P. *Science* **1993**, *260*, 232. (c) Svoboda, K.; Schmidt, C. F.; Schnapp, B. J.; Block, S. M. *Nature* **1993**, *365*, 721. (d) Perkins, T.; Smith, D. E.; Chu, S. *Science* **1994**, *264*, 819. (e) Finer, J. T.; Simmons, R. M.; Spudich, J. A. *Nature* **1994**, *386*, 113.

(4) Quate, C. F. *Surf. Sci.* **1994**, *299/300*, 980.

(5) Hues, S. M.; Colton, R. J.; Meyer, E.; Güntherodt, H.-J. *MRS Bulletin* **1993**, *18*, 41.

are an average over large numbers of molecules contained within the ca. 1 mm^2 probing area. On the other hand, force microscopy, which involves measuring the forces on a sharp tip as it is scanned over a sample, has proven to be a useful tool for imaging the structure and dynamics of surface adsorbates at the nanometer scale.[4-24] Few studies have, however, exploited the exquisite force sensing and imaging capabilities of force microscopes to probe the interactions between molecules and macromolecules.[15-23]

A systematic force microscopy study of interactions between molecular groups requires a flexible methodology for attaching molecules to the probe tip. One successful method that we have recently reported[17] involves self-assembly of functionalized organic thiols onto the surfaces of Au-coated Si$_3$N$_4$ probe tips (Figure 1). Stable and rugged monolayers of alkyl thiols or disulfides containing a variety of terminal groups can be readily prepared[25] and enable systematic studies of the interactions between basic chemical groups on the probe tip and similarly modified Au substrates. Covalent modification of force probes with thiols and reactive silanes has also been reported by other groups in studies of adhesion[19,20] and contact potential.[21] In addition, nonspecific adsorption has been used to study binding between protein−substrate pairs[22,23] and long-range forces between hydrophobic surfaces.[24]

(6) Mate, C. M.; McClelland, G. M.; Erlandsson, R.; Chiang, S. *Phys. Rev. Lett.* **1987**, *59*, 1942.

(7) Burnham, N. A.; Colton, R. J. *J. Vac. Sci. Technol. A* **1989**, *7*, 2906.

(8) (a) Marti, O.; Ribi, H. O.; Drake, B.; Albrecht, T. R.; Quate, C. F.; Hansma, P. K. *Science* **1988**, *239*, 50. (b) Frommer, J. *Angew. Chem., Int. Ed. Engl.* **1992**, *31*, 1298.

(9) Rugar, D.; Hansma, P. K. *Phys. Today* **1990**, *43*, 23.

(10) (a) Ducker, W. A.; Senden, T. J.; Pashley, R. M. *Nature* **1991** *353*, 239. (b) Ducker, W. A.; Senden, T. J. *Langmuir* **1992**, *8*, 1831. (c) Biggs, S.; Mulvaney, P. *J. Chem. Phys.* **1994**, *100*, 8501.

(11) (a) Blackman, G. S.; Mate, C. M.; Philpott, M. R. *Phys. Rev. Lett.* **1990**, *65*, 2270. (b) Joyce, S. A.; Thomas, R. C.; Houston, J. E.; Michalske, T. A.; Crooks, R. M. *Phys. Rev. Lett.* **1992**, *68*, 2790. (c) Burnham, N. A.; Dominguez, D. D.; Mowery, R. L.; Colton, R. J. *Phys. Rev. Lett.* **1990**, *64*, 1931.

(12) (a) Haugstad, G.; Gladfelter, W. L.; Weberg, E. B.; Weberg, R. T.; Weatherill, T. D. *Langmuir* **1994**, *10*, 4295. (b) Radmacher, M.; Fritz, M.; Cleveland, J. P.; Walters, D. A.; Hansma, P. K. *Langmuir* **1994**, *10*, 3809.

(13) Radmacher, M.; Fritz, M.; Hansma, H. G.; Hansma, P. K. *Science* **1994**, *265*, 1577.

(14) Cai, H.; Hillier, A.; Franklin, K. R.; Nunn, C. C.; Ward, M. D. *Science* **1994**, *266*, 1551.

(15) (a) Overney, R. M.; Meyer, E.; Frommer, J.; Brodbeck, D.; Luthi, R.; Howald, L.; Guntherodt, H.-J.; Fujihira, M.; Takano, H.; Gotoh, Y. *Nature* **1992**, *395*, 133. (b) Overney, R. M.; Meyer, E.; Frommer, J.; Guntherodt, H.-J.; Fujihira, M.; Takano, H.; Gotoh, Y. *Langmuir* **1994**, *10*, 1281.

(16) (a) Hoh, J. H.; Cleveland, J. P.; Prater, C. B.; Revel, J. P.; Hansma, P. K. *J. Am. Chem. Soc.* **1992**, *114*, 4917. (b) Weisenhorn, A. L.; Maivald, P.; Butt, H.-J.; Hansma, P. K. *Phys. Rev. B* **1992**, *45*, 11226.

(17) Frisbie, C. D.; Rozsnyai, L. F.; Noy, A.; Wrighton, M. S.; Lieber, C. M. *Science* **1994**, *265*, 2071.

(18) Lee, G. U.; Chrisey, L. A.; Colton, R. J. *Science* **1994**, *266*, 771.

(19) Nakagawa, T.; Ogawa, K.; Kurumizawa, T.; Ozaki, S. *Jpn. J. Appl. Phys.* **1993**, *32*, L294.

(20) Green, J.-B. D.; McDermott, M. T.; Porter, M. D.; Siperko, L. M., submitted for publication.

(21) Thomas, R. C.; Tangyunyong, P.; Houston, J. E.; Michalske, T. A.; Crooks, R. M. *J. Phys. Chem.* **1994**, *98*, 4493.

(22) Lee, G. U.; Kidwell, D. A.; Colton, R. J. *Langmuir* **1994**, *10*, 354.

(23) (a) Florin, E. L.; Moy, V. T.; Gaub, H. E. *Science* **1994**, *264*, 415. (b) Moy, V. T.; Florin, E. L.; Gaub, H. E. *Science* **1994**, *266*, 257.

(24) Tsao, Y.-H.; Evans, D. F.; Wennerström, H. *Science* **1993**, *262*, 547.

(25) (a) Nuzzo, R. G.; Allara, D. L.; *J. Am. Chem. Soc.* **1983**, *105*, 4481. (b) Porter, M. D.; Bright, T. B.; Allara, D. L.; Chidsey, C. E. D. *J. Am. Chem. Soc.* **1987**, *109*, 3559. (c) Bain, C. D.; Troughton, E. B.; Tao, Y.-T.; Evall, J.; Whitesides, G. M.; Nuzzo, R. G. *J. Am. Chem. Soc.* **1989**, *111*, 321. (d) Whitesides, G. M.; Laibinis, P. E. *Langmuir* **1990**, *6*, 87. (e) Dubois, L. H.; Nuzzo, R. G. *Annu. Rev. Phys. Chem.* **1992**, *43*, 437. (f) Bain, C. D.; Evall, J.; Whitesides, G. M. *J. Am. Chem. Soc.* **1989**, *111*, 7155. (g) Delamarche, E.; Michel, B.; Kang, H.; Gerber, Ch. *Langmuir* **1994**, *10*, 4103.

Figure 1. Schematic drawing of a CFM setup. The sample rests on a piezoelectric tube, which can be finely moved in x, y, and z. A laser beam is reflected from the backside of the tip into a photodiode to measure two types of tip-surface interactions: When the sample approaches, touches, and is withdrawn from the tip, the tip will move up and down. In response to surface topography, resulting in the atomic force signal. The tip will also rock back and forth in response to friction, yielding the lateral force signal. The inset illustrates the chemically specific interactions presented in this report. A Au-coated, COOH terminated tip contacts the boundary between CH$_3$ and COOH terminated regions of a sample.

Herein we report systematic force microscopy studies of the interactions between different chemical functional groups covalently linked to a force microscope probe tip and sample substrate. Adhesive forces between probe tips and substrates that have been modified with SAMs terminating with COOH, CH$_3$, and NH$_2$ functional groups have been measured in EtOH and H$_2$O solvents. The measured adhesive forces are found to agree with predictions of the Johnson, Kendall, and Roberts (JKR) theory and thus show that the observed interactions correlate with the surface free energy. In addition, lateral force imaging studies demonstrate that the friction force between different functional groups correlates directly with the adhesion forces between these same groups. The dependence of friction forces on the tip and sample functionality is shown to be the basis for chemical force microscopy in which lateral force images are interpreted in terms of a spatial distribution of different functional groups.

Experimental Section

Materials. Di-11-(4-azidobenzoate)-1-undecyl disulfide, **I**, and 11-mercaptoundecanoic acid were used from previous studies.[17] Octadecanethiol, 3-aminopropyltriethoxysilane, and K(t-Bu)O were available commercially (Aldrich) and used as received. Dioctylamine (Aldrich) was distilled under reduced pressure and stored under N$_2$. The free amine of ethyl-4-aminobutyrate hydrochloride (Aldrich) was obtained by a method adapted from the literature.[26] Briefly, 3 g of the compound was dissolved in the 100 mL of warm EtOH, and 500 mL of Et$_2$O was added, maintaining solubility. Anhydrous NH$_3$ was bubbled through the solution for 30−45 min, and the resulting fine white precipitate was removed by filtration. The remaining clear oil was dried, distilled under reduced pressure, and stored under N$_2$ at 20 °C prior to use. Solvents used in chemical manipulations were of reagent grade or better; solvents used in substrate and probe tip functionalization were HPLC grade to reduce the amount of particulate matter. All water (DI H$_2$O) was deionized with a Barnstead NANOpure II filtration unit to 18 MΩ·cm resistivity.

Au-Coated Substrates and Probe Tips. Substrates of the desired size were cut from Si (100) wafers (Silicon Sense, Nashua, NH; test grade, 500 μm thick). These substrates and commercial Si$_3$N$_4$ tip-cantilever assemblies (Digital Instruments, Santa Barbara, CA) were coated by thermal evaporation (Edwards Auto 306 Cryo evaporator)

(26) Kossel, A. *Hoppe-Seyler's Z. Physiol. Chem.* **1912**, 303.

with a 20 Å adhesion layer of Cr followed by 1000 Å of Au. Care was taken to avoid heating the Si_3N_4 probes during evaporation since it causes the cantilevers to bend. The bending is believed to be due to differences in the thermal expansion coefficients of Au and Si_3N_4. The Au wire (99.99%) was cleaned in 3:1 $HCl:HNO_3$, rinsed with DI H_2O, EtOH, and oven dried immediately prior to evaporation.
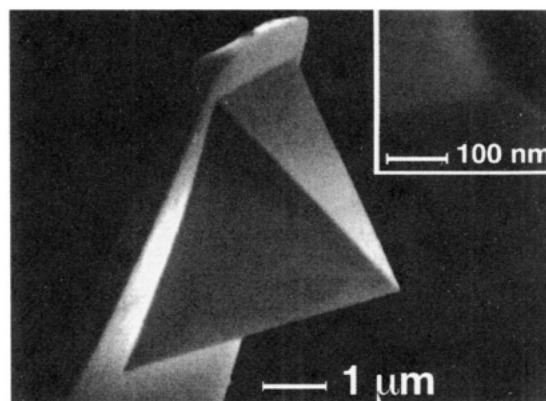
Substrate and Tip Derivatization. Monolayers were formed immediately after Au evaporation. Monolayers of **I** were formed by immersion of the Au samples in 2−3 mM methylcyclohexane solutions for at least 12 h. Monolayers of 11-mercaptoundecanoic acid and octadecanethiol were formed by immersion of the freshly coated substrates and probe tips in 2−3 mM EtOH solutions for at least 2 h. Before use or characterization, all SAM substrates were rinsed in EtOH (SAM substrates of **I** were first rinsed with methylcyclohexane and then EtOH) and dried with a stream of dry Ar. Amine-terminated monolayers were prepared on freshly cleaned Si(100) substrates (1: 1:5 $NH_4OH:H_2O_2:H_2O$, 70 °C, 10 min) using a 2% toluene solution of 3-aminopropyltriethoxysilane. Silane monolayer formation was verified by X-ray photoelectron spectroscopy.

SAM Photopatterning. Amines were covalently attached to Au-**I** SAM substrates in high yield by UV-irradiation as previously reported.[27] SAMs terminating in two distinct functional groups were formed by double irradiation using a mask to define the pattern in the first step. To obtain a patterned surface terminating in a specific array of COOH and CH_3 groups, a drop of ethyl-4-aminobutyrate was first placed on a freshly rinsed and dried Au-**I** substrate. A Cr-on-quartz mask was then placed on top of the substrate, Cr-side down, forcing the amine to spread evenly across the sample. The assembly was irradiated for 2 min through the mask using a filtered (10 cm quartz cell filled with 1:1:1 $H_2O:EtOH:EtOAc$) 200 W Hg lamp ($\lambda > 260$ nm). After rinsing with a copious amount of EtOH and drying with a stream of dry Ar, a drop of dioctylamine was applied to the sample. A clear quartz plate was placed on the sample and the assembly was uniformly irradiated for 2 min, rinsed, and dried.
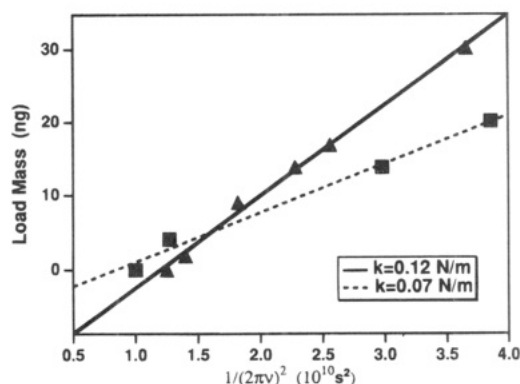
The surface-confined ethyl ester was hydrolyzed following a procedure for the hydrolysis of hindered esters.[28] A solution of 25 mL of ethyl ether, 1.33 mg of K(t-Bu)O, and 60 μL of H_2O was cooled on ice. The solution was transferred to a vial containing the samples and left at room temperature for 2−4 h. Contact angle titration on homogeneous COOH-terminated SAM samples hydrolyzed in this manner were consistent with measurements taken on SAMs of 11-mercaptoundecanoic acid on Au. Condensation figures of the patterned substrates revealed H_2O condensation only on the acid-terminated regions; no H_2O droplets were found on the hydrophobic areas of the sample. Before CFM imaging, the samples were cut to 1.2 cm × 1.2 cm squares, rinsed with DI H_2O, and dried with a stream of dry Ar or N_2. Freshly prepared samples were used for each set of experiments.

Chemical Force Microscopy. Adhesion and friction measurements were made with a Digital Instruments (Santa Barbara, CA) Nanoscope III lateral force microscope (LFM) equipped with a fluid cell. Most measurements were done under absolute EtOH except where noted. Derivatized tips were rinsed in EtOH and dried under N_2 just prior to mounting them in the fluid cell.

Cantilever Calibration. Triangular, 200 μm long Si_3N_4 cantilevers were calibrated using a resonance detection method.[29] Briefly, small endmasses consisting of tungsten spheres (~10 μm diameter, ~4 ng) were placed on the end of the lever using a glass micropipet. The W-spheres stuck to the end of the lever by capillary adhesion. The diameters of the spheres were determined with an optical microscope and used to calculate the added mass. The end-loaded lever was mounted into the scan head of the microscope, and the resonance frequency of thermal vibrations was determined by monitoring the signal from the photodiode detector with a spectrum analyzer (HP-3561A Dynamic Signal Analyzer).

(27) (a) Wollman, E. W.; Kang, D.; Frisbie, C. D.; Lorkovic, I. M.; Wrighton, M. S. *J. Am. Chem. Soc.* **1994**, *116*, 4395. (b) Rozsnyai, L. F.; Wrighton, M. S., submitted for publication in *Langmuir*.

(28) Gassman, P. G.; Schenk, W. N. *J. Org. Chem.* **1977**, *42*, 918.

(29) Cleveland, J. P.; Manne, S.; Bocek, D.; Hansma, P. K. *Rev. Sci. Instr.* **1993**, *64*, 403.

Figure 2. Scanning electron microscopy image of a gold-coated cantilever-tip assembly. The inset shows a high magnification view of the area near the end of the tip.

Figure 3. Plot of the load mass vs $1/(2\pi\nu)^2$. The force constants are 0.07 and 0.12 N/m for native (■) and gold-coated (▲), respectively.

Results and Discussion

Probe Tip Modification. Quantitative interpretation of force microscopy data requires detailed knowledge of the tip radii and spring constants of the gold-coated tip-cantilever assemblies. The tip radius is an important parameter since it affects the tip/ surface contact area (i.e., the number of molecular interactions). A scanning electron microscopy image of a Si_3N_4 cantilever-tip assembly coated with 1000 Å of Au is shown in Figure 2a. No charging effects were observed during SEM imaging, indicating complete Au coating of the tip. Charging did occur on uncoated Si_3N_4 tips. We observed significant variations in radii of curvature for the tips from different batches supplied by the manufacturer. Radii for Au-coated tips range from ~55 nm ("sharp tips", Figure 2) to ~150 nm ("blunt tips"). These differences represent typical variations that can be observed for commercial Si_3N_4 tips obtained from different wafers;[30] the variation of tip radii from a given wafer is, however, much smaller (<10%). Except where noted, all of the adhesion and friction force data presented in this report were taken using the sharp 55 nm tips coated with ~1000 Å of Au and functionalized with the appropriate SAM.
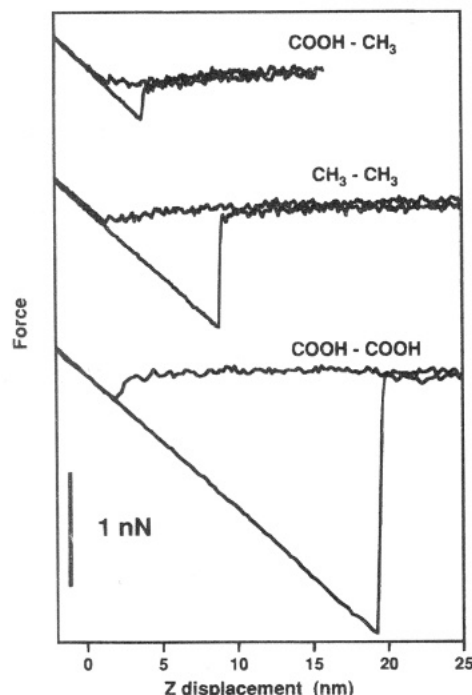
Cantilever force constants, k, have been determined by measuring the cantilever resonance frequency, ν, as a function of the mass of spherical tungsten balls added to the end of the tip.[29] Representative data obtained for both uncoated and Au-coated Si_3N_4 cantilevers are shown in Figure 3. The plots of the added mass versus $1/\nu^2$ yield straight lines with slopes proportional to k. As expected, the thicker Au-coated cantilevers

(30) The variations in tip radius of curvature arise from nonuniformity in the microfabrication steps used to produce the Si_3N_4 catilever-tip assemblies.

Figure 4. Representative force versus displacement curves recorded for (a) COOH/COOH, (b) CH$_3$/CH$_3$ and CH$_3$/COOH tip/sample functionalization using sharp tips ($R \sim 60$ nm.). All data were obtained in EtOH solution using a fluid cell.

exhibit larger force constants ($\sim$0.12 N/m) than the bare Si$_3$N$_4$ cantilevers ($\sim$0.07 N/m). Also, the observed k for the uncoated cantilevers is 40% smaller than that reported by the manufacturer. This deviation represents the typical variation for nominally similar batches of cantilevers and is in agreement with previous reports.[29] Hence, although it is possible to calculate k for the Au-coated cantilevers from the manufacturer's value for the Si$_3$N$_4$ cantilever and the thickness and elastic constants of Au,[31] we have used direct measurements of k in our studies to minimize this source of uncertainty. We also found that the variations in spring constant value for the cantilevers from the same wafer do not exceed 20%[32] and were typically much smaller (i.e., on the order of 10−15%). For this reason we have used an average value of k for cantilevers obtained from the same wafer and Au-coated together in analyzing our experiments.

Adhesive Measurements between Uncharged Functional Groups. The adhesive interaction between different functional groups was determined from force vs cantilever displacement curves. In these measurements the deflection of the cantilever is recorded as the sample approaches, contacts, and is then withdrawn from the probe tip.[33] The observed cantilever deflection is converted into a force using the cantilever spring constant. These measurements were carried out in solution rather than air to eliminate uncertainties arising from capillary forces.[34,35]
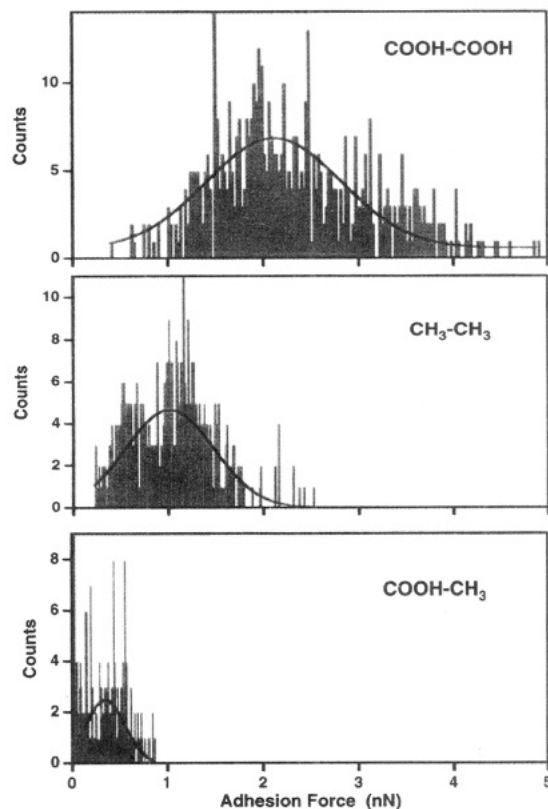
(31) Liu, Y.; Wu, T.; Evans, D. F. *Langmuir* **1994**, *10*, 2241.

(32) The error of ±20% does not exceed the accuracy of the resonance-endmass calibration method. (Cleveland, J. P., personal communication, 1994).

(33) Burnham, N. A.; Colton, R. J.; Pollock, H. M. *J. Vac. Sci. Technol. A.* **1991**, *9*, 2548.

(34) Under ambient conditions the SAM surfaces are covered with thin films of adsorbed H$_2$O and contaminants. These species give rise to relatively large capillary forces that can obscure weak intermolecular interactions.[35] The contribution of capillary forces to measured data can be eliminated by carrying out experiments in ultrahigh vacuum or fluid solution.

(35) Grigg, D. A.; Russel, P. E.; Griffith, J. E. *J. Vac. Sci. Tech. A.* **1992**, *10*, 680.

Figure 5. Histograms showing the number of times that a given adhesion force was observed in repetitive measurements using functionalized samples and sharp tips terminating in (a) COOH/COOH, (b) CH$_3$/CH$_3$, and (c) CH$_3$/COOH. Each histogram represents $\sim$400 repetitive tip-sample contacts for one functionalized tip. All measurements were made in EtOH solution.

Representative force-displacement curves obtained in EtOH using Au-coated tips and samples that were functionalized with SAMs terminating in either CH$_3$ or COOH groups are shown in Figure 4. The hysteresis in the force displacement curves (i.e., approach vs withdrawal) corresponds to the adhesion between functional groups on the tip and sample surface. The magnitude of the adhesive interactions between tip/sample functional groups decreases in the following order: COOH/COOH > CH$_3$/CH$_3$ > CH$_3$/COOH. This observed trend in adhesive force agrees with qualitative expectations that interaction between hydrogen bonding groups (i.e., COOH/COOH) will be greater than non-hydrogen bonding groups (i.e., CH$_3$/CH$_3$). A similar trend is observed for measurements made with blunt tips,[17] although the magnitudes of the adhesion forces are larger by a factor of $\sim$3, owing to the increase in contact area. The ordering of CH$_3$/CH$_3$ and CH$_3$/COOH interactions can also be understood by considering simple free energy arguments as described below.

To quantify the differences and uncertainties in the adhesive interactions between different functional groups, we have recorded multiple force curves ($\geq$300) for each type of intermolecular interaction. These data are plotted as histograms of the adhesive force versus the number of times that this force is observed for the COOH/COOH, CH$_3$/CH$_3$, and CH$_3$/COOH interactions and are shown in Figure 5. The mean value of the interaction, and its experimental uncertainty were determined by fitting the histograms to Gaussian curves. This analysis yields mean adhesive forces ±1σ uncertainties of 2.3 ± 0.8, 1.0 ± 0.4, and 0.3 ± 0.2 nN for the interactions between COOH/COOH, CH$_3$/CH$_3$, and CH$_3$/COOH groups, respectively.[36] Since the mean value for each type of interaction is outside the uncertainty range for the other interactions, these results show

that we can reproducibly differentiate between chemically distinct functional groups by measuring the adhesion force.

In addition, these adhesion data can be used to assess the energetics of the different intermolecular interactions and the absolute number of functional groups that contribute to the experimentally observed forces. We have quantitatively addressed these two points using the JKR theory of adhesion mechanics.[1a,37] The JKR model of adhesion mechanics, which has been well-tested over the past 20 years, predicts that the adhesion force, F_{ad}, or force required to separate a tip of radius R from a planar surface at pull-off is given by

$$F_{ad} = -\frac{3}{2}\pi R W_{st} \qquad (1)$$

where W_{st} is the work of adhesion for separating the sample and tip. The work of adhesion can be estimated by[37]

$$W_{st} = \gamma_s + \gamma_t - \gamma_{st} \qquad (2)$$

where γ_s and γ_t are the surface free energies of the sample and tip, and γ_{st} is the interfacial free energy of the two contacting surfaces. If we consider the sample and tip combinations that have the same surface functional groups (i.e., CH_3/CH_3 and COOH/COOH), then $\gamma_{st} = 0$ and $\gamma_s = \gamma_t$, and it is possible to simplify the eq 2 to $W_{st} = 2\gamma$, where γ in our case corresponds to the free energy of the surface in equilibrium with solvent. Hence, it is simply this surface free energy that should determine the adhesive force between tip and sample covered with the same functional groups.

We have checked the validity of this approach by estimating the expected value of F_{ad} for CH_3 terminated surfaces and tips. Previous measurements of the contact angle of EtOH on CH_3-terminated SAMs[25c] yield a value of $\gamma = 2.5$ mJ/m^2.[38] The value of F_{ad} calculated using this value of γ and the radius of the tip, R,[39] is 1.2 nN, in good agreement with the experimentally determined value of 1.0 nN for sharp tips (see Figure 5). Similar agreement was also found in calculations made using the radii of the blunt tips.[17] These results thus demonstrate that the continuum JKR approach provides a reasonable interpretation of our nanoscopic measurements.

Significantly, the above analysis can also be turned around to yield important information about the free energies of surfaces. Since high free energy surfaces are readily wet by liquids, contact angle measurements cannot be used to extract directly γ_s. This disadvantage turns out to be an advantage in our measurements because high surface energies lead to large adhesion forces that are easily measured. For example, in the case of COOH-terminated SAMs, which are completely wet by EtOH, we found $F_{ad} = 2.3$ nN for the sharp probe tips. The value of γ(COOH) in EtOH obtained using this force and the same tip radius as in the CH_3 calculation is 4.5 mJ/m^2. These values of γ(COOH) and γ(CH$_3$) together with the CH$_3$/COOH

adhesion force also enable us to calculate the value of the interface free-energy: γ_{st}(CH$_3$/COOH) = 5.8 mJ/m^2. This value of γ_{st} readily explains the ordering of intermolecular adhesive forces; that is, the large and unfavorable interface free energy dominates γ(COOH) and γ(CH$_3$) in EtOH and results in a smaller adhesive interaction for CH$_3$/COOH versus CH$_3$/CH$_3$. Lastly, we note that this approach can obviously be extended to other functional group pairs and different solvent systems and that such studies should provide of wealth of useful thermodynamic data to predict for example relative degrees of binding.

In addition, we have used the JKR model to estimate the number of molecular interactions contributing to the measured adhesive forces. The contact radius at pull-off, a_s, for surfaces terminating in the same functional groups is

$$a_s = \left[\frac{3\pi\gamma R^2}{K}\right]^{1/3} \qquad (3)$$

where K is the elastic modulus of the tip and sample. The value of K can be reasonably approximated using the bulk value for gold, 64 GPa, assuming that SAMs do not change significantly the elastic behavior of the solids. For the CH$_3$/CH$_3$ interaction we calculate that $a_s = 1.0$ nm, and thus that the contact area is 3.1 nm^2. This corresponds to an interaction between only 15 molecules on the tip and sample.[1b] Furthermore, if the tip radius was reduced to ~10 nm the contact area at pull-off should correspond to interaction between only single molecular pairs! Measurements in this latter regime could be especially interesting since they would provide truly microscopic data addressing solvated intermolecular interactions and could test for a breakdown of contiuum theories such as JKR.

Electrostatic Interactions. Adhesive interactions between oppositely charged monovalent functional groups have also been investigated. The electrostatic contribution to the attractive and repulsive forces between charged surfaces has been studied previously using the SFA and force microscopy.[2,24,40] These studies have probed the long-range coulombic interactions that occur between two charged surfaces as they approach one another. In the present study, we were concerned with the role that electrostatic interactions play as two surfaces just separate (i.e., the contribution to adhesion), rather than the effects at long distances.

To study this electrostatic interaction we utilized monolayers of 11-mercaptoundecanoic acid on the probe tip and 3-amino-propyltriethoxysilane on a Si substrate. Simple amines and carboxylic acids are well-known to be ionized in aqueous solutions under neutral conditions. Although the pK_a's of acidic and basic groups on SAM surfaces shift by approximately 2 pH units higher and lower, respectively,[41] they still should be ionized in solution. Histograms of the adhesion force recorded in deionized H$_2$O (18 MΩ·cm) at pH = 6.5 and in 0.3 M NaCl solution (pH = 6.5) using blunt (~150 nm) tips are shown in Figure 6. The mean adhesive force between these oppositely charged groups is 14 nN in H$_2$O, but decreases to 4.5 nN in 0.3 M NaCl. This salt concentration reduces the characteristic length scale (i.e., the Debye length, λ_D) for the electrostatic interaction to only 5.5 Å (vs ~1 μm in deionized H$_2$O).[1a] Along with the significant drop in the length scale of the interaction we found that the adhesive force drops by a factor of three to 4.5 nN. The strong decrease in the measured force with increasing ionic strength suggests that in pure H$_2$O a significant component of the total force arises from charge—charge

(36) The Gaussian fits are believed to provide a good means for estimating the uncertainty in these experiments but may not represent the best model for fitting this type of data (Noy, A.; Lieber, C. M. unpublished results). For example, the Gaussian fit assumes a symmetric distribution of forces between ±∞, while all forces are >0.

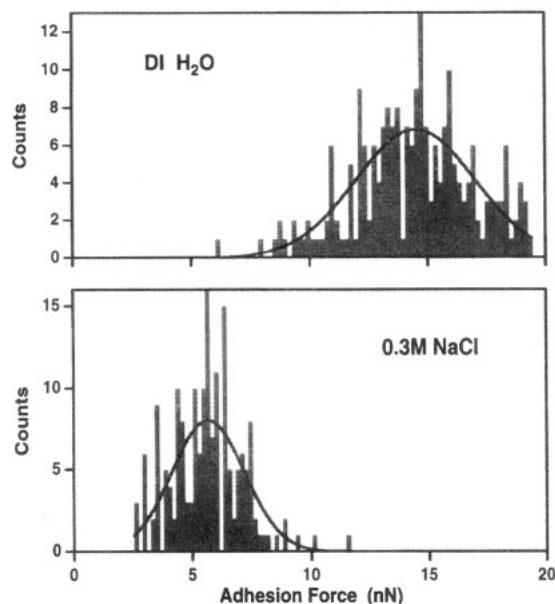(37) Johnson, K. L.; Kendall, K.; Roberts, A. D. *Proc. R. Soc. London, A.* **1971**, *324*, 301.

(38) Adamson, A. W. *Physical Chemistry of Surfaces*; John Wiley & Sons: New York, 1990.

(39) The radius of the tip (R_t) determined from the analysis of electron microscopy images is 60 nm. The value of R used in eq 1 is, however, reduced by the effective curvature of the gold islands that make up the sample surface (R_s). We have measured R_s to be approximately 500 nm by contact AFM.

$$R = R_t R_s / R_t + R_s = 54 \text{ nm}$$

(40) Butt, H.-J. *Biophys. J.* **1991**, *60*, 1438.

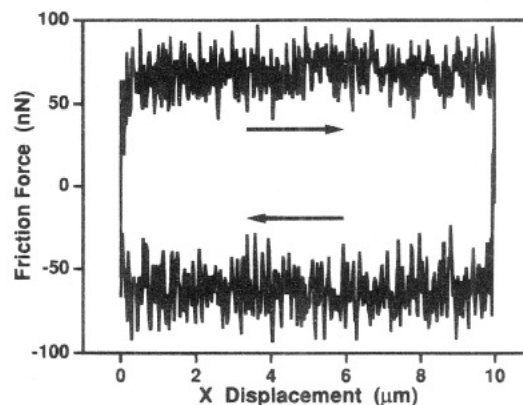(41) Lee, T. R.; Carey, R. I.; Biebuyck, H. A.; Whitesides, G. M. *Langmuir* **1994**, *10*, 741.

Figure 6. Histograms of force vs displacement curves recorded between functionalized samples terminating in NH_3^+ groups and tips terminating in COO^- groups in (a) DI H_2O (18 MΩ·cm) at pH = 6.5 and (b) 0.3 M NaCl aqueous solution at pH = 6.5.
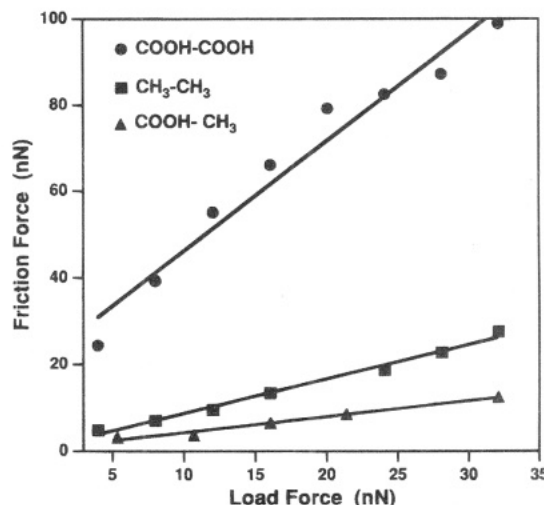
interactions between groups outside of the area of physical contact between the tip and sample.[42] To probe further the interactions between the amine- and carboxyl-terminated SAMs in aqueous solution we have also investigated the pH dependence of the adhesive force.[43] These measurements demonstrate at low pH, where the acid and amine are both protonated (i.e., a uncharged/positively charged interaction), that the adhesive interaction is much smaller than at neutral pH. Likewise, at high pH, where the acid and amine are deprotonated (i.e., a negatively charged/uncharged interaction), we find that adhesive force is again much smaller than at neutral pH. These results support our hypothesis that the large magnitude of the adhesive force at neutral pH arises from a charge−charge interaction and, furthermore, suggest pH dependent measurements of the adhesive force as an approach for local measurements of pK's of ionizable groups at surfaces.

Friction Measurements and Imaging. Recently, we proposed that friction and adhesive forces between structurally similar SAMs should correlate directly with each other since microscopically both forces originate from the breaking of intermolecular interactions.[17] To test quantitatively this hypothesis we have studied the friction force between functional groups on a sample surface and tip by recording the lateral deflection of the tip cantilever, while the sample was scanned in a forwards/backwards cycle along the x-direction. The resulting curve is called a friction loop (Figure 7).[44] The values of the lateral force plotted in these loops were determined from the lateral spring constant of the cantilever and lateral sensitivity of the optical detector in our force microscope.[29,45] The friction force corresponds to one half of the difference between upper and lower lateral forces plotted in the loop.

Friction loops were recorded and analyzed as a function of the applied load and the functional groups terminating the surface and tip SAMs. Data recorded with sharp tips are

(42) (a) Derjaguin, B. V.; Muller, V. M.; Toporov, Yu, P. *J. Coll. Interfac. Sci.* **1975**, *53*, 314. (b) Maugis, D. *J. Coll. Interfac. Sci.*, **1992**, *150*, 243.
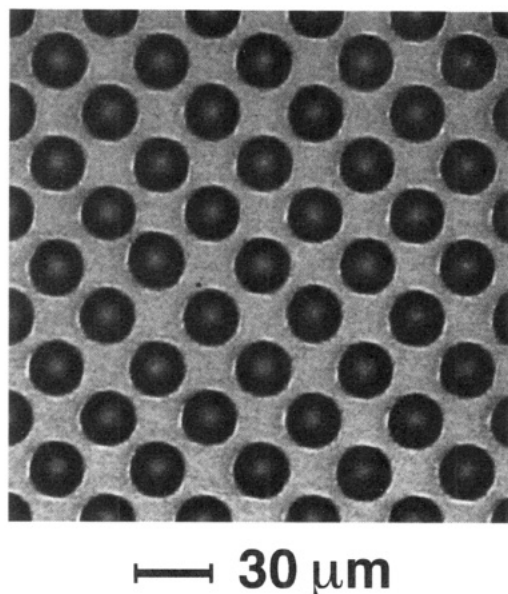(43) Noy, A.; Vezenov, D.; Rozsnyai, L. F.; Wrighton, M. S.; Lieber, C. M., manuscript in preparation.
(44) Overney, R. M.; Takano, H.; Fujihira, M.; Paulus, W.; Ringsdorf, H. *Phys. Rev. Lett.* **1994**, *72*, 3546.

Figure 7. A typical friction loop recorded on a COOH terminated sample using COOH modified probe tip in EtOH solution. Applied load was 17 nN.

Figure 8. Summary of the friction force vs applied load data recorded for functionalized samples and tips terminating in COOH/COOH (●), CH_3/CH_3 (■), and COOH/CH_3 (▲) in EtOH.

summarized in Figure 8. We found that the friction force increases linearly with the applied load for each combination of chemically modified tip and surface and that for a fixed applied load the friction force decreases as follows: COOH/COOH > CH_3/CH_3 > COOH/CH_3. Similar trends were observed for data recorded with blunt tips, although again, the magnitude of the friction values were larger due to the greater contact areas.[46] The coefficients of friction (μ), which were determined from the slopes of friction vs load plots, are 2.5, 0.8, and 0.4 for COOH/COOH, CH_3/CH_3, and COOH/CH_3 interactions, respectively. Notably, the trend in the magnitudes of the friction forces and coefficients (Figure 8) is the same as

(45) The lateral spring constant, k_{lat}, for a triangular cantilever is

$$k_{lat} = \frac{2}{6\cos^2\theta + 3(1+\nu)\sin^2\theta}\left(\frac{L}{H}\right)^2 k_n$$

where θ is the angle between the base arms of the triangular cantilever, ν is the Poisson ratio for Si_3N_4, L is the length of the cantilever beam, H is the length of the tip, and k_n is the normal spring constant (For the derivation of this formula, see Appendix). Substituting the measured values of k_n, L, H, and θ, and the literature value of ν (*CRC Handbook of Materials Science*, *v.II*; Lynch, C. T., Ed.; CRC Press: Boca Raton, FL, 1975; p 382) yields $k_{lat} = 225$. This value is similar to that reported in previous studies.[15]

(46) The contact radius, a, for an applied load of F is given by

$$a^3 = \frac{R}{K}[F + 3\pi RW_{12} + (6\pi RW_{12}F + (3\pi RW_{12})^2)^{1/2}]$$

where R is the tip radius. Hence, as the tip radius increases the contact area and number of intermolecular interactions will increase for a given applied load.

that observed for the adhesion forces (Figure 5): COOH/COOH terminated tips/samples yield large friction and adhesion forces, while COOH/CH_3 functionalites yield the lowest friction and the smallest adhesion.

These new results confirm our earlier suggestion[17] that the friction and adhesion forces between structurally similar but chemically distinct SAMs correlate directly with each other. In contrast, SFA studies of different hydrocarbon surfactants found that the friction force correlated with adhesion hysteresis and not the adhesion force.[2b,47] These studies focused on stucturally disimilar phases (i.e., cystalline, amorphous, and liquid-like) and thus differ from the present studies in which the structurally similar (crystalline[48]) SAMs were probed. More recent SFA studies of stucturally similar layers show, however, that friction force correlates with the force of adhesion.[49] In addition, independent force microscopy studies[20] have recently observed results similar to our investigations. Hence, we believe that this is a manifestation of a general relationship between adhesion and friction on a microscopic scale.[50]

The differences in friction shown in Figure 8 can also be exploited to produce lateral force images of patterned surfaces with predictable contrast. Using the photochemical method described above we have produced SAMs having 10 μm × 10 μm square regions that terminate with COOH groups and repeat every 30 μm in a square pattern; the regions of the SAM surrounding these hydrophilic squares terminate with hydrophobic CH_3 groups (Figure 9). Figure 10 shows topography and lateral force images of the patterned SAMs recorded using tips modified with SAMs terminating in either COOH or CH_3 groups. The surface exhibits a flat topography across the CH_3 and COOH terminated regions of the sample (Figure 10a). Though several small adventitious particles are detected on the sample surface, no chemical information is revealed. Figure 10b shows a friction map of the same area as in Figure 10a, and here chemical information about the surface is readily apparent. Friction maps recorded with the COOH terminated tips exhibit high friction (light color) in the square area of the sample that contains the COOH terminated SAM and low friction in the CH_3 terminated regions (Figure 10b). Images recorded with CH_3 terminated tips exhibit a reversal in the friction contrast: low friction (dark color) in the square area of the sample that contains the COOH terminated SAM and higher friction over the surrounding CH_3 terminated regions (Figure 10c). Note that the contrast in Figure 10b is greater than that in Figure 10c. This difference in friction contrast is consistent with the friction vs load curves obtained on homogenous SAM samples (see Figure 8). Namely, at a given applied load the difference in friction between the two surface functionalities

├─── **30 μm**

Figure 9. Condensation image of H_2O on a photopatterned SAM substrate showing the repeat pattern of 10 × 10 μm^2 squares terminating in COOH on a background terminating in CH_3. H_2O condenses only on the hydrophilic COOH-terminated regions of the sample.

obtained with a COOH tip is always greater than the difference between the same two groups obtained with a CH_3-terminated tip.

The reversal in image (friction) contrast occurs only with changes in the probe tip functionality, and thus we can conclude that we are imaging with sensitivity to chemical functional groups. For this reason we have previously called this approach to imaging (i.e., with specifically functionalized tips) chemical force microscopy.[17] Predictable image contrast using chemically derivatized tip has also been observed in a recent independent study,[20] and thus we believe this approach is clearly reproducible and may serve as a method for mapping more complex and chemically heterogeneous surfaces. The image resolution at present is not a single functional group but rather an ensemble of groups defined by the tip contact area (see above). The resolution in this study is limited by the resolution of the surface photopatterning and does not represent the resolution limit of the technique. Other researchers have previously used differences in friction forces to map different domains of phase segregated Langmuir−Blodgett films.[15] The image contrast in this work, however, is believed to be due to differences in the elastic properties of the domains and not the chemical functionality at the film surface.[15b]

Lastly, the friction force on these patterned SAMs has also been determined in air. We find that "acid-tip contrast" (*i.e.*, high friction in the hydrophilic regions of the surface) is always observed in air regardless of whether the tip is bare Si_3N_4, coated with Au, or derivatized with COOH or CH_3 functional groups. Similar images of patterned SAMs using unmodified Si_3N_4 tips have been reported by Whitesides and co-workers.[51] The mechanism of contrast in these images is not unambiguously determined but is likely due to differences in capillary forces in the hydrophilic and hydrophobic portions of the surface. Capillary forces are typically 10 times stronger than the adhesion forces that were measured in EtOH[35] and will thus overwhelm small differences in the intermolecular interactions in air.[52] Force microscopy studies in solution not only eliminate this problem

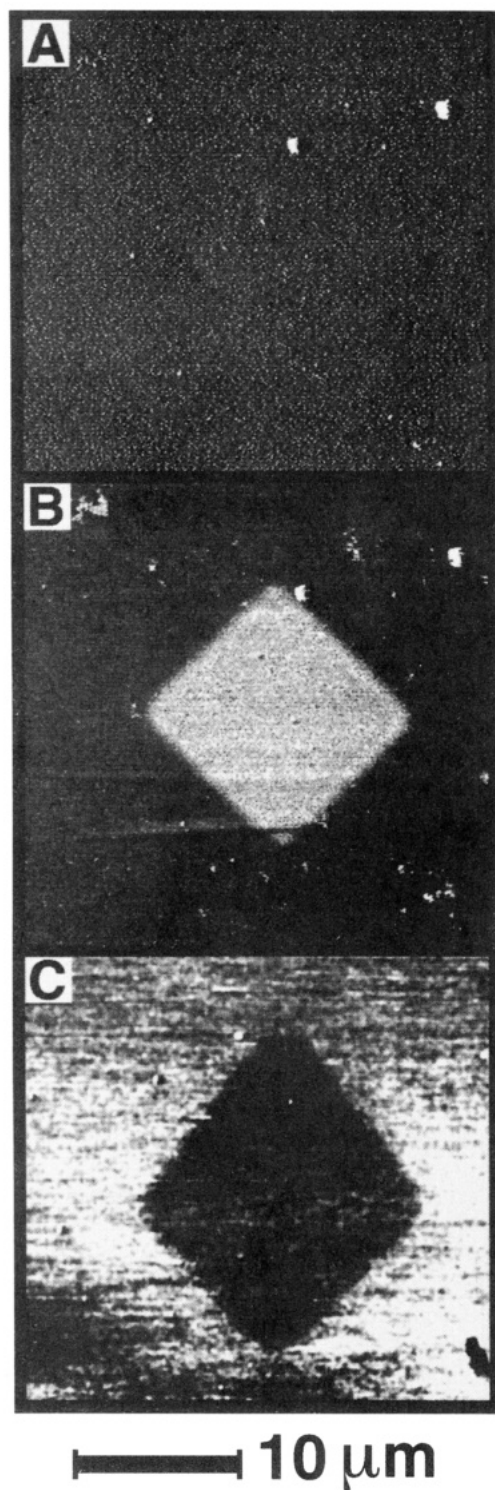(47) Chaudhury, M. K.; Owen, M. J. *Langmuir* **1993**, *9*, 29.

(48) Adhesion and friction force measurements were made with samples composed of homogeneous long-chain alkylthiols which have crystalline structure (see ref 25). In the case of functional group imaging, SAMs terminating in a relatively bulky phenylazide group were used, and the desired terminal groups were subsequently attached photochemically. Though the same trend in friction is observed in these SAMs as with the simpler homogeneous monolayers, the same argument for crystalline structure cannot be made.

(49) Yoshizawa, H.; Israelachvili, J. *Thin Solid Films* **1994**, *246*, 71.

(50) It is important to recognize, however, several caveats that must be considered in making comparisons of friction data obtained with functionalized surfaces and tips. First, similar radii tip must be used since the friction force depends on contact area.[46] Secondly, the surface solvation must be controlled since the capillary force can dominate other contributions. In this regard, we believe that imaging in solution or ultrahigh vacuum represent the only unambiguous controls of the surface solvation (i.e., an uncontrolled layer of adsorbates such as H_2O will be present on a surface even in inert atmosphere conditions).

(51) Wilbur, J. L.; Biebuyck, H. A.; MacDonald, J. C.; Whitesides, G. M. *Langmuir* in press.

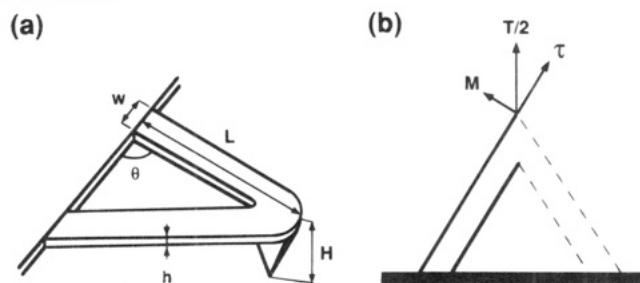(52) Binggeli, M.; Mate, C. M *Appl. Phys. Lett.* **1994**, *65*, 415.

Figure 10. Force microscopy images on one square of a photopatterned sample identical to that shown in Figure 9; the images are of (a) topography, (b) friction force using a tip modified with a COOH-terminated SAM, and (c) friction force using a tip modified with a CH₃-terminated SAM.

but also are most relevant to stucture and function determination of chemical, biological, and materials systems. We believe that our approach will prove useful to these latter areas in the future.

Conclusions

We have shown that molecules may be attached to Au-coated force microscope probe tips using the well established affinity of thiols for Au, and that the chemically modified tips produced

Scheme 1

(a) **(b)**

by this method may be used to quantitatively measure adhesion and friction forces between the functional groups terminating the SAMs on a tip and sample. Adhesion studies between SAMs which terminate with COOH and CH₃ functional groups have shown that the interaction between COOH/COOH > CH₃/CH₃ > COOH/CH₃. These adhesion forces agree well with forces predicted by the JKR theory of adhesive contact. Using this model we were also able to show that the contact area between sharp (~60 nm) tips and the sample corresponds to an interaction between only 15 molecular pairs and that by reducing the tip radii to ~10 nm it may be possible to measure the interactions between single molecular pairs. Our analyses of these data also show how it should be possible using CFM to determine surface free energies for organic surface/liquid interfaces that are unobtainable by contact angle measurements.

In addition, the friction force between tips and samples modified with COOH and CH₃ groups has also been measured as a function of applied load. The magnitude of the friction force was found to be COOH/COOH > CH₃/CH₃ > COOH/CH₃, thus demonstrating that friction forces between different chemical functional groups correlate directly with adhesion forces between the same groups. The predictable dependence of friction forces on the tip and sample functionality was further shown to be the basis for chemical force microscopy where lateral force images are interpreted in terms of the strength of adhesive interactions between functional groups.

We also believe that these studies open up significant areas of research for the future. For example, (1) a host of different types of molecular interactions can be studied since the modification of probe tips with SAMs provides a general way to introduce chemical functionality onto probe tips; (2) basic thermodynamic information that will be relevant to chemists and biologists can be extracted from the analysis of CFM data obtained in different solvent media; and (3) CFM imaging of other systems (e.g., polymers and biomolecules) could lead to new insights into the spatial distribution of functional groups and/or hydrophobic vs hydrophilic domains.

Appendix

Calculation of the Lateral Spring Constant for a V-shaped Cantilever. A V-shaped cantilever can be approximated by two identical rectangular beams made of a material with Young's modulus E, shear modulus G, and Poisson ratio ν. If the total torque applied to the cantilever (Scheme 1) is T, then the torque

applied to one of the beams is $T/2$. Also the strain energy stored in one beam is equal to one-half of the total strain energy, SE.

The beam length width and height are denoted respectively as L, w, and h. The angle between cantilever beam and the substrate is θ. Let M and τ be the bending and twisting components of torque. The strain energy stored in one beam is:

$$\frac{1}{2}\text{SE} = \int_0^L \frac{M^2}{2EI}dx + \frac{\tau^2 L}{2GJ} = \frac{M^2 L}{2EI} + \frac{\tau^2 L}{2GJ} =$$

$$\frac{\dfrac{T^2}{4}L\cos^2\theta}{2E\left(\dfrac{1}{12}wh^3\right)} + \frac{\dfrac{T^2}{4}L\sin^2\theta}{2\left[\dfrac{E}{2(1+\nu)}\right]J} \quad (A1)$$

where I and J are the moments of inertia for a rectangular beam. For the case when $w \gg h$ expressions for J and I are[31]

$$I = \frac{wh^3}{12}$$

$$J = \frac{wh^3}{16}\left(\frac{16}{3} - 3.36\frac{h}{w}\right) \approx \frac{wh^3}{3} \quad (A2)$$

Therefore, total strain energy is:

$$\text{SE} = 2\left[\frac{1}{2}\frac{T^2}{4}L\left(\frac{\cos^2\theta}{\dfrac{1}{12}wh^3 E} + \frac{\sin^2\theta}{\dfrac{1}{3}wh^3 G}\right)\right] =$$

$$\frac{T^2 L}{2Ewh^3}[6\cos^2\theta + 3(1+\nu)\sin^2\theta] \quad (A3)$$

The torsional spring constant k_t can be obtained as a reciprocal of the second derivative of the total strain energy with respect to T

$$k_t^{-1} = \frac{\partial^2(\text{SE})}{\partial T^2} \quad (A4)$$

Therefore

$$k_t = \frac{Ewh^3}{L}\left[\frac{1}{6\cos^2\theta + 3(1+\nu)\sin^2\theta}\right] \quad (A5)$$

The values of h and E are not well-known and may vary

significantly due to poor reproducibility of the materials growth process. Therefore, we have related the value of k_t to the experimentally determined normal spring constant, k_n. For a V-shaped tip, k_n can be approximated as a sum of normal spring constants for two rectangular beams[31]

$$k_n = 2 \times \frac{3EI}{L^3} = \frac{Ewh^3}{2L^3} \quad (A6)$$

Then the ratio for the torsional spring constant to normal spring constant would be

$$\frac{k_t}{k_n} = \frac{\dfrac{Ewh^3}{L}\left[\dfrac{1}{6\cos^2\theta + 3(1+\nu)\sin^2\theta}\right]}{\dfrac{Ewh^3}{2L^3}} =$$

$$\frac{2L^2}{[6\cos^2\theta + 3(1+\nu)\sin^2\theta]} \quad (A7)$$

The torsional spring constant can be converted to the lateral spring constant k_{lat} (related to lateral displacement) according to the following formula

$$k_{lat} = \frac{k_t}{H^2} \quad (A8)$$

where H is the tip vertical height. Therefore, the final formula for the lateral spring constant of a V-shaped cantilever-tip assembly is

$$k_{lat} = \frac{2}{[6\cos^2\theta + 3(1+\nu)\sin^2\theta]}\left(\frac{L}{H}\right)^2 \times k_n \quad (A9)$$

The only elastic parameter that this formula contains is the relatively well-known Poisson ratio for silicon nitride.[45] All other parameters can be determined directly by measurement.